Effect of pH on the Synthesis of $LiCoO_2$ with Malonic Acid and Its Charge/Discharge Behavior for a Lithium Secondary Battery

Do-Hoon Kim, Euh-Duck Jeong,[1] Sang-Pil Kim,[2] and Yoon-Bo Shim*

Department of Chemistry and Chemistry Institute for Functional Materials, Pusan National University, Pusan 609-735, Korea
Received June 2, 2000

The pH effect of the precursor solution on the preparation of $LiCoO_2$ by a solution phase reaction containing malonic acid was carried out. Layered $LiCoO_2$ powders were obtained with the precursors prepared at the different pHs (4, 7, and 9) and heat-treated at 700 °C ($LiCoO_2$-700) or 850 °C ($LiCoO_2$-850) in air. pHs of the media for precursor synthesis affects the charge/discharge and electrochemical properties of the $LiCoO_2$ electrodes. Upon irrespective of pH of the precursor media, X-ray diffraction spectra recorded for $LiCoO_2$-850 powder showed higher peak intensity ratio of I(003)/I(104) than that of $LiCoO_2$-700, since the better crystallization of the former crystallized better. However, $LiCoO_2$ synthesized at pH 4 displayed an abnormal higher intensity ratio of I(003)/I(104) than those synthesized at pH 7 and 9. The surface morphology of the $LiCoO_2$-850 powders was rougher and more irregular than that of $LiCoO_2$-700 made from the precursor synthesized at pH 7 and 9. The $LiCoO_2$ electrodes prepared with the precursors synthesized at pH 7 and 9 showed a better electrochemical and charge/discharge characteristics. From the AC impedance spectroscopic experiments for the electrode made from the precursor prepared in pH 7, the chemical diffusivity of Li ions (D_{Li^+}) in $Li_{0.58}CoO_2$ determined was 2.7×10^{-8} cm^2s^{-1}. A cell composed of the $LiCoO_2$-700 cathode prepared in pH 7 with Lithium metal anode reveals an initial discharge specific capacity of 119.8 $mAhg^{-1}$ at a current density of 10.0 mAg^{-1} between 3.5 V and 4.3 V. The full-cell composed with $LiCoO_2$-700 cathode prepared in pH 7 and the Mesocarbon Pitch-based Carbon Fiber (MPCF) anode separated by a Cellgard 2400 membrane showed a good cycleability. In addition, it was operated over 100 charge/discharge cycles and displayed an average reversible capacity of nearly 130 $mAhg^{-1}$.

Introduction

$LiCoO_2$ as a cathode material for a lithium ion battery has received much attention,[1-6] after Sony Co. introduced a lithium-ion battery consisting a $LiCoO_2$ cathode and a carbon anode at 1990s. Many studies[3-8] have been carried out for the preparation of $LiCoO_2$, electrochemical characterizations, etc. to obtain superior charge/discharge properties. $LiCoO_2$ is usually prepared by employing a solid phase reaction, where the oxide/carbonate salts of cobalt and lithium were treated at a high temperature for several hours after a mechanical mixing of the compounds. On the other hand, the solid phase reactions have disadvantages, such as non-homogeneity of particles with abnormal grain growth and poor control of stoichiometry. The solution phase reaction is preferable to overcome the above disadvantages and to lower the synthesis temperature of the precursor that leads to get a good $LiCoO_2$ in homogeneous with smaller grain size. We previously reported a low temperature synthesis of homogeneous $LiCoO_2$ powders by solution phase reactions by employing the complex formation reaction between humic acid and cobalt and/or lithium ions in an aqueous solution using a sol-gel process. Ogihara *et al.*[10] dissolved $LiNO_3$ and $Co(NO)_3 \cdot 6H_2O$ in an aqueous solution, and treated this solution with mist generated by an ultrasonic vibrator at 900 °C. The specific capacity obtained from the solution phase reaction was about 80-110 mAh/g and this is comparable to one that was resulting from other solid phase reactions using carbonates. However, there was some attention to the solution phase reaction for the preparation of $LiCoO_2$,[11-17] although several groups reported on the preparation of lithium manganese oxides in a solution phase reaction of sol-gel processes.[17-19]

In the present study, we have synthesized $LiCoO_2$ powders by a solution phase method containing malonic acid at various pHs. The solution phase reaction causes the powder to be homogeneous with small particles and the growth was affected by the pH of precursor synthesis media. Malonic acid possesses two carboxylic acid groups that can form complexes with metal ions. Generally, the complexation ability of the acid type ligand depends on the pH of the media, due to the different degree of dissociation. Thus, the physical properties of the resulting powder of $LiCoO_2$ synthesized in different pHs of the precursor media might differ from each other. By having the above in mind, we compared the electrochemical and charge/discharge characteristics of the $LiCoO_2$ powders prepared from the precursors synthesized at pH 4, 7, and 9. To characterize the $LiCoO_2$ cathode made from the precursors synthesized at different pH conditions, the electrochemical experiments were performed using cyclic voltammetry, charge/discharge experiment, and AC

*To whom correspondence should be addressed. E-mail: ybshim @hyowon.pusan.ac.kr; Fax: +82-51-516-7421
[1]Present address: Pusan branch of Korea Basic Science Institute.
[2]Present address: Saehan Industrials Ltd.

impedance spectrometry at various experimental conditions. Besides that XRD, TG/DSC, and SEM studies were performed to confirm its composition, structure, and morphology of powders synthesized at different pHs. Cycling test for a full-cell was also carried out under the constant current mode.

Experimental Section

Preparation of the $LiCoO_2$ precursor. 0.2 mole of malonic acid (Aldrich Co.) was dissolved in 100 mL water purified by a Milli-Q system (18 MΩ). First, a 100 mL aqueous solution containing 0.2 mol $LiOH \cdot H_2O$ was added to the malonic acid solution with stirring until the completion of reaction at room temperature. The metal complex precursor was finally prepared by adding a 100 mL aqueous solution containing 0.2 mol $Co(NO)_3 \cdot 6H_2O$ to the above solution at pH 4, pH 7, and pH 9, which were adjusted by using NH_4OH and HCl solutions. The precursor was obtained as a gel type followed by concentrating and evaporating the mixture solution on a hot plate. The gel was ignited in a furnace for 6 hrs at 350 °C, then for 12 hrs at 450 °C. The final $LiCoO_2$ powder was obtained by heating the precursor twice at 700 °C or 850 °C in a tube type furnace under the stream of air.

Preparation of the electrode and the cell. The cathode was prepared by coating the following mixtures on a current collector. The mixture was made of 85%(w/w) $LiCoO_2$ powder, 10%(w/w) acetylene black, and 5%(w/w) polyvinylidene fluoride (PVDF) dissolved in *n*-Methyl pyrrolidone (NMP). The mixture was coated on the current collector of 1 cm^2 stainless steel No. 316 ex-met by tape casting followed by the evaporation of the NMP. It was then dried under vacuum for 24 hrs at 120 °C. The weight of each electrode was at 20-25 mg. Lithium metal ribbon (Aldrich Co.) pressed on a stainless-steel No. 316 ex-met was used as both counter and reference electrodes. A cell composed of the $LiCoO_2$ working, lithium counter, and reference electrodes were used in a 1.0 M $LiClO_4$/propylene carbonate (PC) solution (Battery grade from Mitsubishi Petrochemical Co.) under Ar gas atmosphere at room temperature. A glass cell assembly was used to record cyclic voltammograms (CVs) and AC impedance spectra, and two electrodes system was used for galvanostatic charge/discharge experiments. The charge/discharge test for an actual lithium ion battery was undertaken for a cylindrical type electrode with the size of 50×500 mm^2. The cell consisted of $LiCoO_2$-700 or $LiCoO_2$-850 cathodes, and the MPCF (Mesocarbon Pitch-based Carbon Fiber, PETOCA Co.) anode in an EC/DEC (50% volume ratio) solution containing 1.0 M $LiPF_6$ (Merck Co.).

Instruments. Thermogravimetric analysis (TGA) was performed at the heating increment of 10 °C/min up to 900 °C in air by using a Seiko Instrument Analyzer (Model SSC/5200 SII). X-ray diffraction (XRD) analyses of the $LiCoO_2$ powder were carried out using a Rigaku X-ray diffractometer (D/Max) with a CuK_α (1.5405 Å) radiation source monochromated with a Ni-filter at the scanning range from 10° to 80° (+2 θ). Scanning electron microscopic pictures for $LiCoO_2$ electrodes were obtained from Hitachi Co. Model S-2400 Scanning Electron Microscope (SEM). Cyclic voltammograms were recorded by employing a PAR Model 273 Potentiostat/Galvanostat (EG & G Co.) with Kipp & zonen X-Y recorder. Experiments for specific capacity versus cyclability, properties of charge/discharge, and open circuit voltage (OCV) experiments were carried out using a PAR 363 Potentiostat/Galvanostat interfaced with an IBM-compatible personal computer using an in-house software program. The AC impedance measurements were carried out using a PAR Model 273A Potentiostat/Galvanostat (EG & G Co.) coupled with an EG & G 5201 Lock-in amplifier. Impedance spectra were recorded under the potentiostatic control of the cell voltage and the galvanostatic measurements were carried out by applying an AC voltage of 5 mV-rms amplitude over the frequency range from 100 kHz to 1 mHz after the electrode attaining equilibrium potential. The impedance spectrometer was controlled by an IBM-compatible personal computer, and the data were analyzed in terms of an equivalent circuit by using software supplied by EG&G PAR. The full cells cycling performance was done with a series 2000 Charge-Discharge Tester (MACCOR Co.) interfacing with an IBM-compatible computer in a glove box (VAC Co.)

Results and Discussion

TGA and XRD patterns of $LiCoO_2$ precursors synthesized at various pHs. The thermal analysis technique gives the optimum heat-treatment temperature required to prepare the $LiCoO_2$ powder was determined for the precursors synthesized in different pHs media. Figure 1 shows TGA curves recorded for the starting materials for the precursor syntheses. TGA curve recorded for $LiOH \cdot H_2O$(a), which is one of the starting material for the preparation of the $LiCoO_2$ precursor, shows weight losses of 41.68% and 9.78% at 60-100 °C and 550-630 °C, respectively due to its degradation to H_2O and OH^-. At around 630-740 °C a 22.70% in weight was increased due to the formation of Li_2O. In the case of

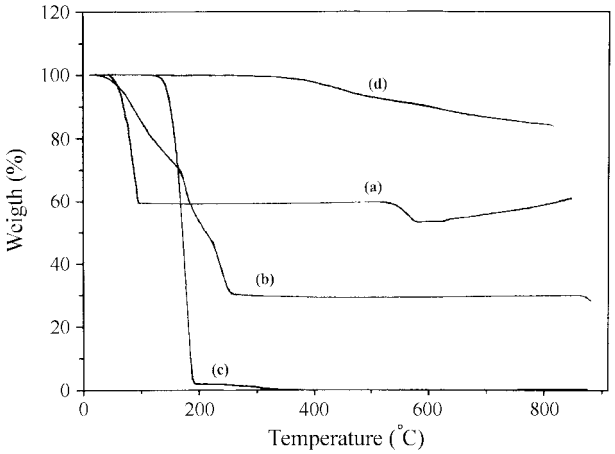

Figure 1. TGA curves recorded for the related compounds to the precursor synthesis; (a) $LiOH \cdot H_2O$, (b) $Co(NO_3) \cdot 6H_2O$, (c) malonic acid, and (d) $LiCoO_2$.

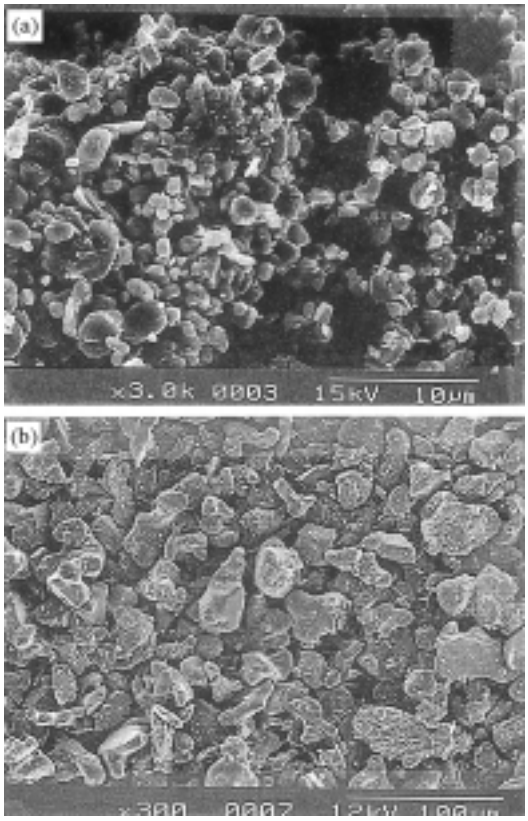

Figure 2. SEM photographs of $LiCoO_2$ powders synthesized at pH 7. (a) 700 °C, (b) 850 °C.

$Co(NO_3) \cdot 6H_2O$(b), the total weight loss observed was 73.72%, and the one of occurred at 60-122 °C was 17.86%, and another at 170-250 °C was 43.33% due to the degradation to H_2O and NO_3^-. TGA curve for malonic acid(c) shows a 98.06% degradation at around 160-200 °C. All starting materials were degraded to H_2O and CO_2 in prior to 600 °C. In addition to that the precursors synthesized respectively at pH 4, 7, and 9 showed the TG curves with similar weight losses. Since there are no signals indicating the formation of Li_2O at 700 °C in the TGA curves recorded for $LiCoO_2$(d). Hence, it was assumed that all the precursors were crystallized to $LiCoO_2$. These results showed that the solution phase reaction results in a lower heat-treatment temperature for the $LiCoO_2$ precursor.

SEM photographs of $LiCoO_2$ were obtained for the powders synthesized in an aqueous medium of pH 7, followed by the heat-treatment separately at 700 °C and 850 °C as shown in Figure 2(a) and (b), respectively. The size of grains prepared at 700 °C was nearly 1 mm, and another prepared at 850 °C was several times larger grain size than that of 700 °C. Particle size of $LiCoO_2$ treated at 850 °C were different from each other in different pHs of synthesizing media, which were about 40, 29, 45 μm for pH 4, 7, and 9, respectively. It suggests that the particle size was not dependant to the pH of the precursor media but to the heat-treat temperature. The surface morphology of all the particles was smooth, but powders prepared at 850 °C were rather rougher and irregular than that of at 700 °C. The morphology was different from each other, depending on the pH of the solution. In addition, the particle size of the powder prepared at pH 4 was larger and less homogenous than that prepared at pH 7 or 9. The dissociation constants (pK_{a1} and pK_{a2}) of malonic acid are 2.8 and 5.7, respectively. This means that dissociation of the acid is incomplete at pH 4. Thereby, the formation of homogenous $LiCoO_2$ precipitates via the complex formation reaction would be relatively more difficult below pH 5.7. On the other hand, the homogenous precipitates can be obtained over pH 7, which is due to the higher value than the pK_{a2}.

Table 1 shows the observed lattice parameters of $LiCoO_2$ powders synthesized at pH 4, 7, and 9, such as *a* and *c* values, line intensities of I(003) and I(104), and *a*/*c* ratio. The Miller indices indicate that the powder has a pure hexagonal structure with a $R\bar{3}m$ space group. Generally, the (003) line intensity decreases when a metal (M) atom partially occupies a part of the octahedral sites of the Li layer in $LiMO_2$ (M=Co, Ni, V, and Cr). In the present study, the strongest peak was observed at the miller index (003) in all samples of $LiCoO_2$-700 and $LiCoO_2$-850. The latter had a little stronger intensity of the (003) line than the former. This indicates that the degree of the crystallization of the powder was higher when prepared at 850 °C than that did at 700 °C. However, the electrochemical performances for the former were better. For $LiCoO_2$-700 °C, d values for (003), (101), and (104) lines moved slightly to the lager one as the pH of synthesizing media went to higher pHs. Especially, $LiCoO_2$ synthesized at pH 4 displayed larger intensity ratios of I(003)/I(104) than those synthesized at pH 7 and 9. The electrochemical characteristics of $LiCoO_2$ synthesized at pH 4 were

Table 1. Lattice parameters calculated from XRD data of $LiCoO_2$ heat-treated at 700 °C and 850 °C

Parameter Temp. & pH		d value (Å)			Lattice parameters (hexagonal)		*c*/*a*	Intensity ratio of I(003)/I(104)
		(003)	(101)	(104)	*a* (Å)	*c* (Å)		
700 °C	pH 4	4.657	2.396	1.999	2.806	13.97	4.979	1.55
	pH 7	4.682	2.402	2.003	2.815	14.05	4.989	1.14
	pH 9	4.684	2.403	2.003	2.816	14.05	4.991	1.03
850 °C	pH 4	4.706	2.408	2.007	2.822	14.12	5.003	10.12
	pH 7	4.696	2.408	2.006	2.827	14.04	4.992	6.17
	pH 9	4.679	2.401	2.003	2.814	14.04	4.988	8.02

poor. This means that the shift in d value and abnormally larger intensity ratios of I(003) and I(104) shows that it affect to lithium insertion/deinsertion processes. Gummow et al.[4] had reported that the crystal structure of the $LiCoO_2$ powder was depend on the heat treatment temperature. Thus, the abnormal intensity ratios of I(003)/I(104) for the powder obtained at 850 °C from the precursor synthesized at pH 4 might have a distorted structure. In the present study, the XRD patterns of the powder were slightly different from each other depending on the heat treatment temperature. The lithium and cobalt layers of $LiCoO_2$ prepared with precursors synthesized at pH 7 and 9 are well spaced in the rock salt structure, indicating that well-crystallized $LiCoO_2$ can be obtained even at a lower heat-treatment temperature when compared to the other reports.[3,5,7,9]

Cyclic Voltammetric and charge/discharge behavior of the $LiCoO_2$ electrode. The CVs recorded for the $LiCoO_2$ electrodes, which were prepared with the precursor synthesized using malonic acid in different pH media (pH 4, pH 7, and pH 9) and heat-treated at the low temperature (700 °C), show only one set of redox peaks being independent on the pH (see Figure 3(a)). The peak potentials of the $LiCoO_2$ prepared at pH 4, 7, and 9 were 4.01 V/3.85 V, 4.02 V/3.86 V, and 4.00 V/3.87 V at the scan rate of 0.01 mV/sec, which did not change according to the pH of the preparing solution. CVs recorded for $LiCoO_2$-700 electrodes prepared used with the precursor synthesized at pH 4, 7, and 9 show a set of well-separated redox peaks. However, the anodic peak currents are larger than that of the corresponding cathodic one. This indicates that the redox process is not fully reversible and the lithium ions that de-intercalated at a higher potential than 4.0 V are irreversibly re-intercalated during the cathodic process. This made the initial charge/discharge efficiency lower. This behavior may be due to that as the lithium ions are de-intercalated from the $LiCoO_2$ crystal and Co^{3+} oxidized to Co^{4+}, which increases the concentration of Co^{4+} in $LiCoO_2$ at high potentials. In addition, one set of redox peaks appearing in the CV recorded for the $LiCoO_2$-700 electrode indicates that it has a single-phase transition process during charge/discharge between 3.0 and 4.4 V. Here, the lithium intercalation and de-intercalation reactions are also a one-step process.

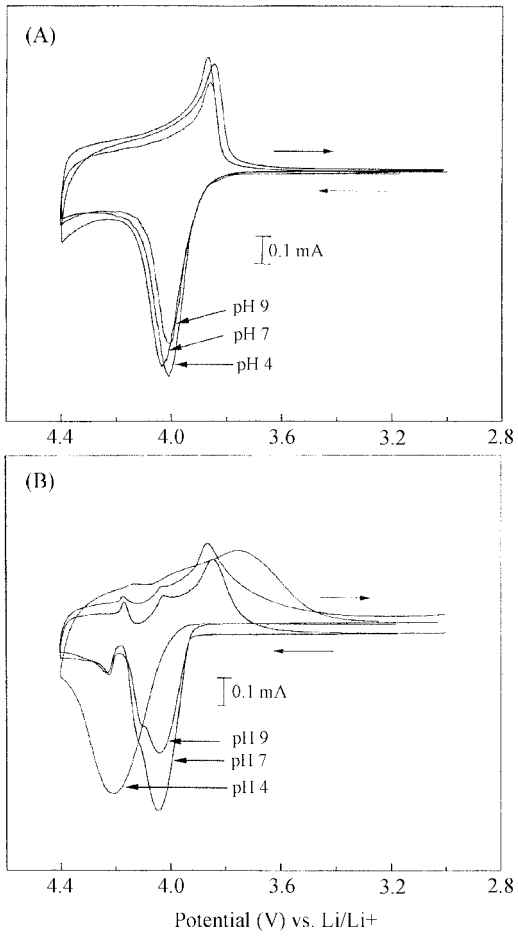

Figure 3. Cyclic voltammograms of $LiCoO_2$ electrodes prepared at different pHs and heat-treatment in 1M $LiClO_4$/PC at 0.01mV/sec; heat treated at (a) 700 °C and (b) 850 °C. The potential range was 3.0 V- 4.4 V *vs*. Li/Li^+.

While, the CV recorded for the electrodes treated at 850 °C (Figure 3(b)) shows three redox peaks as like the $LiCoO_2$ electrodes synthesized in the solid phase reaction except that the electrode prepared the precursor synthesized at pH 4. Three redox peaks in the CV must be a result of the phase transitions, and/or cation disorders in the structure. Exceptionally, the electrode prepared with the $LiCoO_2$ powder made up of the precursor synthesized at pH 4 and heat treated at 850 °C shows only one anodic peak at 4.25 V and a large cathodic peak at 3.75 V and very large peak separation compared with that obtained at pH 7 and 9 (see Figure 3(b)). This indicates that the electrode prepared with the precursor synthesized at pH 4 and heat-treated at 850 °C has different electrochemical properties when compared to that obtained from pH 7 an 9. The CV recorded for the electrode prepared at 850 °C shows smaller cathodic peaks than anodic ones, which were independent on pHs of precursor synthesis media.

To investigate the effects of the heat-treated temperature using the precursors synthesized at various pH conditions of the precursor preparing media on the charge/discharge characteristics, the charge-discharge experiments between 4.2 and 3.6 V were undertaken with a $LiCoO_2$/Li cell at 0.4 mA/cm^2 (see Figure 4). Large decrease in the discharge capacity was observed for the electrodes prepared with the powder that was synthesized at pH 4 and heat-treated at 700 °C and 850 °C. While, the decrease of the discharge capacity was slow for the electrodes obtained at pH 7 and 9. This means that charge/discharge characteristics did not depends on the heat-treated temperature, but on the pH of synthesis media of the precursor. It is due to the difference of the complex formation ability that affects the oxide formation according to pH. Thus, The charge/discharge efficiency was good for the electrode made of $LiCoO_2$ powders synthesized at pH 7 and 9, which is due to the complete complexation to be given homogeneous particles at low temperature.

OCV patterns of the $LiCoO_2$ electrodes. Charge/discharge characteristics of $LiCoO_2$ powders, which were prepared with malonic acid at pH 7 and 9 were better than those

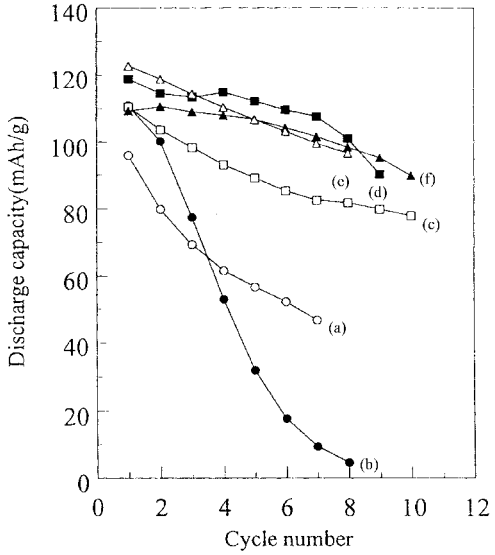

Figure 4. Variation of discharge capacities as a function of cycle number for $LiCoO_2$ electrode at a current density of 0.4 mA/cm^2 in 1 M $LiClO_4$/PC. (a) 700 °C-pH 4, (b) 850 °C-pH 4, (c) 700 °C-pH 7, (d) 850 °C-pH 7, (e) 700 °C-pH 9, and (f) 850 °C-pH 9.

prepared at pH 4. $LiCoO_2$ prepared at pH 4 shows a poor cycle ability and charge/discharge properties, while properties of the $LiCoO_2$ powders prepared at pH 7 were similar to that prepared at pH 9. This agrees with the CV results, in which the reversibility of the redox reaction in the CV was good for $LiCoO_2$ prepared at pH 7 and 9. For $LiCoO_2$ prepared at pH 4, charge/discharge experiment between 4.2 and 3.6 V at the current density of 0.4 mA/cm^2 shows a decrease in the discharge capacity that was larger than those prepared at pH 7 and 9.

Figure 5 presents the first galvanostatic intermittent charge curves at the charging capacity of 0-180 mAh/g recorded for (a) $LiCoO_2$-700 and (b) $LiCoO_2$-850 electrodes which were prepared with the powder synthesized at pH 7. The cell was charged for a given time, then the current was stopped and it

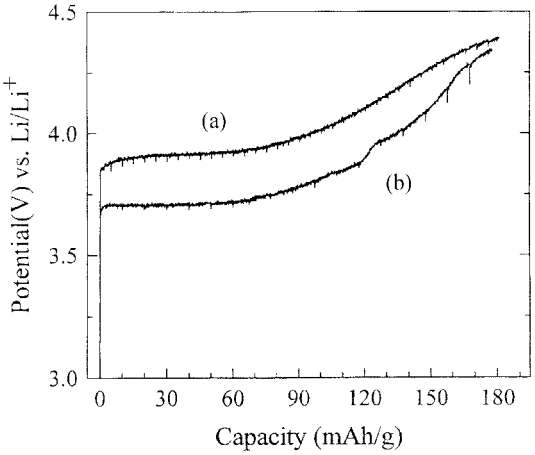

Figure 5. The first galvanostatic intermittent charge curves in Li/1M $LiClO_4$ in PC. (a) 700 °C-pH 7 and (b) 850 °C-pH 7. The current density was 10 mA/g.

was allowed to relax. By applying a constant current (10mA/g) to the cell for 1800 sec during charging, the open circuit voltage recorded for 600 sec varied as shown in Figure 5. Both the $LiCoO_2$-700 and $LiCoO_2$-850 electrodes showed a two-phase reaction until 90 mAh/g charging state, $Li_{0.67}CoO_2$.[5,11] After this, the former has no potential plateau and indicating a lithium-ion diffusion proceed in a single phase. The latter has two potential plateaus due to the phase transition, as reported by Reimer and Dahn.[3] This result is consistent with the CV result that the $LiCoO_2$-700 and $LiCoO_2$-850 electrodes showed one and three redox peaks, respectively.

Impedance spectroscopic behavior of the $LiCoO_2$ electrode. The previous data shows that the electrode made up of the precursor synthesized at pH 7 was best. Thus, we performed the impedance spectrometry for the electrode prepared with the precursor synthesized at pH 7. Figure 6(A) shows a Nyquist plot for a $LiCoO_2$-850 (pH 7) electrode at various cathodic potentials (intercalation processes of lithium ions) from 4.3 to 3.2 V *vs.* Li/Li$^+$ electrode. In order to

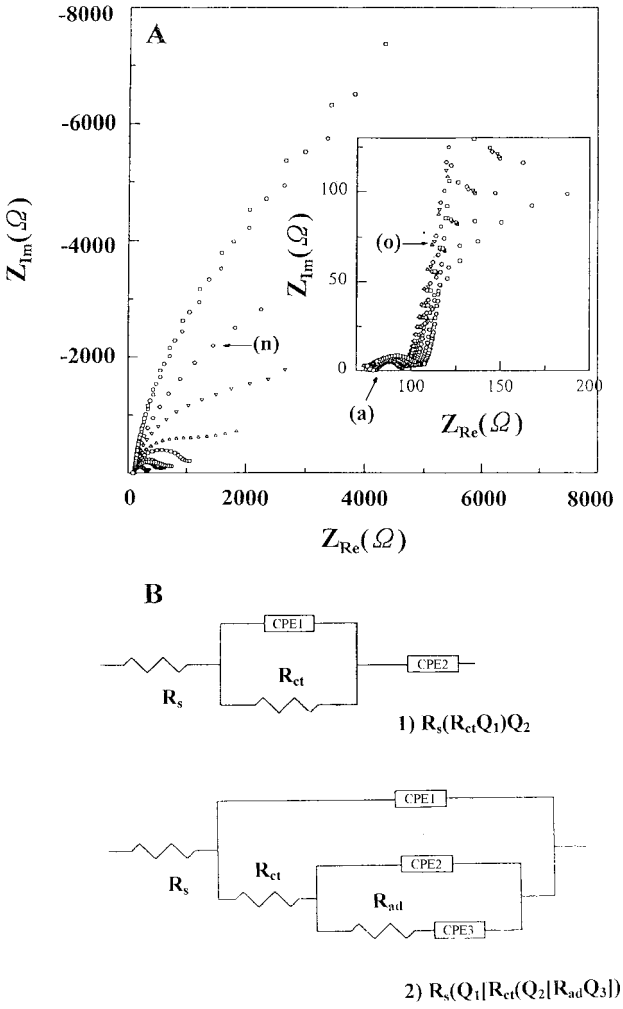

Figure 6. (A) Nyquist plots obtained for the $LiCoO_2$ (850 °C-pH 7) electrode at various applied reduction potentials. (a) 4.30 V. (b) 4.20 V, (c) 4.15 V, (d) 4.10 V, (e) 4.05 V, (f) 4.0 V, (g) 3.95 V, (h) 3.90 V, (i) 3.85 V, (j) 3.80 V, (k) 3.70 V, (l) 3.65 V, (m) 3.60 V, (n) 3.40 V, and (o) 3.20 V *vs.* Li/Li$^+$. Measuring frequency range = 100 kHz-1 mHz. (B) Equivalent circuits for CNLS-fitting.

Table 2(a). Values of the parameters of the equivalent circuit simulated for the impedance spectra of $LiCoO_2$ (850 °C-pH 7) electrode recorded in the positive voltage direction

1) $R_s(Q_1R_{ct})Q_2$ 2) $R_s(Q_1[R_{ct}(Q_2[R_{ad}Q_3])])$

Oxidation potential, V	R_s Ω	R_{ct} Ω	Q_1		R_{ad} Ω	Q_2		C	Q_3		Remark
			Yo, mho × 10^{-6}	n_1		Yo, mho × 10^{-3}	n_2		Yo, mho	n_3	
3.20	79.62	13.31	16.27	0.8714	–	59.71	0.3295	9.425	–	–	1)
3.40	79.62	13.31	16.27	0.8714	–	59.71	0.3295	9.425	–	–	"
3.80	78.67	13.17	16.04	0.6580	–	–	–	–	–	–	"
3.90	78.93	16.61	10.98	0.6750	365.7	18.21	0.8532	–	0.1284	0.7393	2)
3.95	77.29	16.98	14.51	0.6485	61.84	18.09	0.7899	–	0.1819	0.7583	"
4.00	80.29	15.54	95.33	0.7078	43.51	17.31	0.7927	–	0.2234	0.7368	"
4.05	79.73	14.78	74.90	0.7405	30.91	15.90	0.7857	–	0.6889	0.5307	"
4.10	81.21	14.70	66.40	0.7574	31.03	15.30	0.8064	–	0.6709	0.6008	"
4.20	79.65	14.22	71.54	0.7548	33.28	14.60	0.8002	–	0.2795	0.4630	"
4.25	80.09	14.45	84.49	0.7386	42.49	14.15	0.8417	–	0.2248	0.4496	"
4.30	80.61	16.32	14.87	0.6629	65.61	14.70	0.8780	–	0.4230	0.5614	"

Table 2(b). Values of the parameters of the equivalent circuit simulated for the impedance spectra of $LiCoO_2$ (850 °C-pH 7) electrode recorded in the negative voltage direction

1) $R_s(Q_1R_{ct})Q_2$ 2) $R_s(Q_1[R_{ct}(Q_2[R_{ad}Q_3])])$

Oxidation potential, V	R_s Ω	R_{ct} Ω	Q_1		R_{ad} Ω	Q_2		Q_3		Remark
			Yo, mho × 10^{-6}	n_1		Yo, mho × 10^{-3}	n_2	Yo, mho × 10^{-3}	n_3	
4.30	80.35	14.18	31.17	0.83	1740	2.30	1	54.89	0.39	2)
4.20	80.10	14.59	39.98	0.79	322.1	22.4	1	58.55	0.42	"
4.15	79.10	15.49	51.33	0.76	332.8	22.8	1	54.27	0.45	"
4.10	79.58	15.72	48.06	0.77	360.9	21.8	1	61.22	0.41	"
4.05	77.29	16.17	55.61	0.76	395.7	21.0	0.99	65.77	0.41	"
4.00	77.29	16.82	55.30	0.76	435.0	20.8	0.99	67.94	0.40	"
3.90	75.88	22.32	107.0	0.66	802.5	20.0	0.96	88.26	0.50	"
3.80	76.62	23.72	116.0	0.67	–	15.6	0.90	–	–	1)
3.70	77.00	25.28	137.9	0.65	–	15.5	0.91	–	–	"
3.40	79.39	29.09	162.5	0.63	–	1.90	0.93	–	–	"
3.20	77.94	30.05	12.89	0.66	–	1.10	0.93	–	–	"

interpret the impedance spectra, we described an equivalent circuit derived from a CNLS (complex non-linear least square) fitting analysis. The circuits shown in Figure 6(B) in which two equivalent RC circuits are present to describe the impedance responses shown in Figure 6(A). The impedance spectra were analyzed with the "Equivalent Circuit" software provided by the Universiteit Twente through EG&G by working out appropriate equivalent circuits and fitting to the experimental data. Here CPEs stand for constant phase elements.

From 3.8 V to the open circuit voltage, impedance spectra display an arc, an inclined line, and a normal line to x-axis at the region of high, middle, and low frequencies, respectively. The arc and lines correspond to the charge transfer resistance (R_{ct}) and diffusion and charge saturation processes.[20] As the applied potential goes from 4.3 to 3.8 V, which is around the peak potential in the CV, the second arc in the higher frequency range begins to appear from the set-up potential of the CV (as shown in Figure 3). It corresponds to the resistance caused by another charge-transfer process (R_{ad}) that is due to insertion/extraction of Li ions in the interface of the electrolyte/oxide electrode. While, the inclined line in the lower frequency range below 20 mHz is attributable to the Warburg impedance (CPE3), where the charge transfer is controlled by the diffusion of lithium ions through the $LiCoO_2$ electrode. The R_{ad} of the second arc gradually increased with decreasing the applied potentials (the lithium intercalation process), because of increasing the resistance of the adsorption layer formed on the electrode surface by accumulation of lithium.[21,23,24] Impedance spectra for a $LiCoO_2$ electrode at various oxidation potentials (de-intercalation process of lithium ions) with a variation from 3.2 to 4.3 V *vs*. Li/Li^+ electrode are similar to the spectra recorded for the above reduction process, except for small differences in the values. Results of the equivalent circuit analysis during the anodic process are listed in Table 2. As the applied potential goes to the anodic direction, the second arcs in the higher frequency range begin to appear from the set-up potential (3.9 V), which is around the peak potential in the CV. The R_{ad} of the second arc gradually decreased with

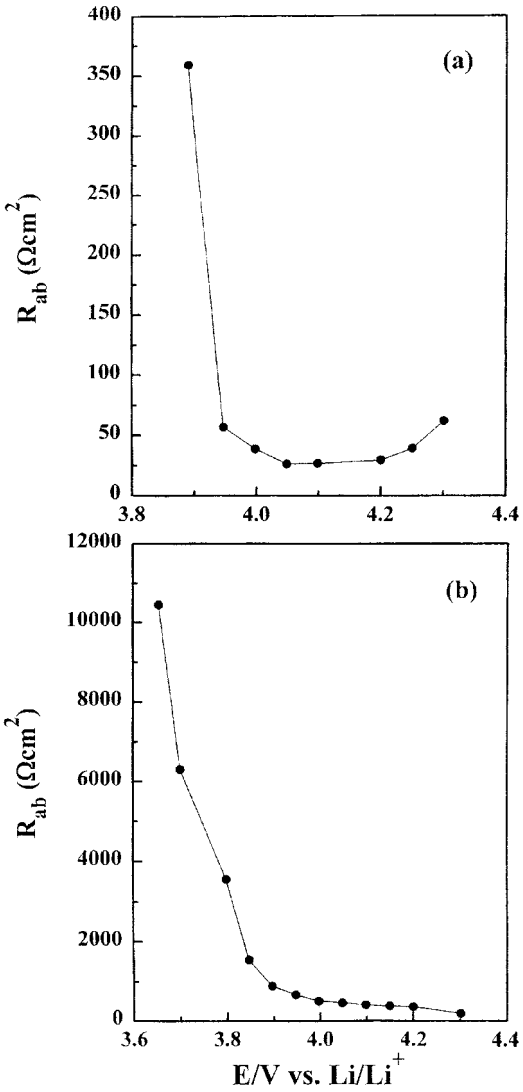

Figure 7. Variation of adsorption resistance, R_{ad}; association with electrochemical lithium intercalation/de-intercalation reactions into the $LiCoO_2$ electrode in 1M $LiClO_4$ in PC solution with (a) de-intercalation process (anodic direction) and (b) intercalation process (cathodic direction).

increasing the applied potentials to the electrode because de-intercalation inducts electrostatic repulsion of oxygen layers, thereby, the lattice expansion allows to reduce the internal resistance.

Figure 7 shows that the resistance, R_{ad}, fluctuation according to the potential variation. R_{ad} values gradually decrease as the applied oxidation potential goes from 3.95 V to 4.2 V. This means that lithium ions easily come out from the inside the electrode during the de-intercalation process (Figure 7 (a)) when compared with the process being inserted into the electrode during the intercalation process (Figure 7(b)). As previously mentioned, this result is in consistent with the CV results and that shows a decrease in the internal resistance of the electrode at the potentials beyond the oxidation peak. While, a higher internal resistance in the lower oxidation potential region is attributable by increasing internal resistance with large degrees of lithium ions intercalation. This

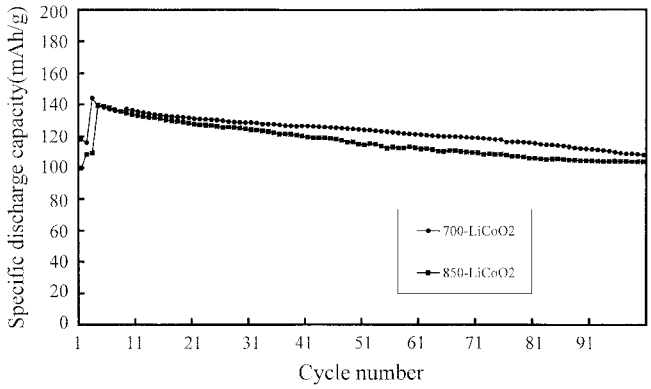

Figure 8. Specific discharge capacities of a full cell composed of the carbon (MPCF) anode and the $LiCoO_2$ cathode separated by Cellgard 2400 using an electrolyte of 1.0 M $LiPF_6$ in an EC/DEC (1 : 1) solution.

behavior is similar to that for $LiCo_yNi_{1-y}O_2$ and $LiMn_2O_4$ electrodes previously reported.[25] However, this result is different from that of a $LiCoO_2$ thin layer electrode of Nishima *et al.*[26] They reported that the electrode had only one semicircle on impedance spectra. A Nyquist plot at a constant charge/discharge current was similar to the result obtained at various potentials (not shown).

To determine the chemical diffusivity of the $LiCoO_2$, D_{Li}^+, the data from Figure 6, which have Q_3 values of the range from 0.4 to 0.5 (See Table 2(b)) indicating the presence of Warburg impedance, was used to plot CNLS fitting. Therefore, the value of the chemical diffusivity, D_{Li}^+, in $LiCoO_2$ was calculated by using the Eq. (1).[22]

$$D_{Li}^+ = \pi f_T r^2/1.94 \quad (1)$$

Where, f_T is the frequency at the transition from the semi-infinite diffusion behavior to finite-length diffusion behavior, and r is the average radius of the $LiCoO_2$ particles. Its values were obtained by the SEM analysis. Here, the chemical diffusivity of $Li_{0.58}CoO_2$ (4.2 V) was determined to be $2.7 \times 10^{-8}\ cm^2s^{-1}$.

The cycling performance of the full-cell composed of MPCF/$LiCoO_2$. To represent an actual battery system, the cycling performance was investigated for a full cell composed of the carbon (MPCF) anode and the $LiCoO_2$ cathode separated by Cellgard 2400 using an electrolyte of 1.0 M $LiPF_6$ in an EC/DEC (1 : 1) solution (see Figure 8). The cycling tests were performed between the potential range of 4.2 V and 2.7 V at a charge and discharge current density of 100 mA/g and 50 mA/g, respectively. Figure 8 illustrates the specific discharge capacity as a function of the number of cycles for $LiCoO_2$-700 and $LiCoO_2$-850 cathodes using the precursor synthesized at pH 7. Although the curve of the $LiCoO_2$-700 exhibited a similar form compared with that of the $LiCoO_2$-850, the performance of the $LiCoO_2$-700 was better than that of the $LiCoO_2$-850 cathode. The average discharge voltages of these systems are above 3.6 V. As the number of cycles increases, the discharge capacity gradually decreases by around the 100th cycle (see Figure 8). The discharge energy decreases to 77% and 74% of the initial value

for the $LiCoO_2$-700 and $LiCoO_2$-850, respectively at 100 cycling. In this case, the coulombic efficiency was 98-99%.

Conclusions

The CVs, charge/discharge data indicates that single-phase $LiCoO_2$ powders with fine and well-developed layered structure can be synthesized by an aqueous complex formation reaction using malonic acid. The pH of the media for the synthesis of the precursor affects the crystal structure and electrochemical properties of the $LiCoO_2$ powder due to the incompleteness of the complex formation reaction at the lower pHs than the pK_{a2} value of the ligand. The $LiCoO_2$-700 made of the precursor synthesized at pH 7 gave an excellent CV cycling behavior at the potential range between 3.0 V and 4.4 V *vs*. Li/Li^+ electrode. It shows only one redox peak due to a single-phase transition, whereas the $LiCoO_2$-850 gave three redox peaks due to a complex phase-transitions and/or cation disorders on the structure. These results are consistent with the OCV curve patterns. From the AC impedance studies, the resistance due to the adsorption of lithium ions into oxide electrode was gradually decreased with increasing the applied potentials to the electrode. The chemical diffusivity of the lithium ions in $Li_{0.58}CoO_2$ synthesized at pH 7 in the present study was calculated to be 2.7×10^{-8} cm^2s^{-1}. The charge and discharge capacity of the lithium ion battery, which composed of the $LiCoO_2$-700 (synthesized at pH 7) cathode and carbon (MPCF) anode, were 119.8 and 117.9 mAh/g, respectively at the first cycle. While the number of cycles increase to 100, the discharge capacity dropped to 91% of the first cycle, having the charge/discharge efficiency of 98-99%. The performance of the $LiCoO_2$-700 electrode was better than that of the $LiCoO_2$-850 electrode in this work, which was obtained from the CV and OCV studies.

Acknowledgment. Grant from the Korean Science and Engineering Foundation (No. 961-0304-030-2) and BK21 program supported this work.

References

1. Brandt, K. *Solid State Ionics* **1994**, *69*, 173.
2. Nagaura, T. *JEC Battery Newsletter* **1991**, *2*, 17.
3. Reimer, J. N.; Dahn, J. R. *J. Electrochem. Soc*. **1992**, *139*, 2091.
4. Gummow, R. J.; Thackeray, M. M.; David, W. I. F.; Hull, S. *Mat. Res. Bull*. **1992**, *27*, 327.
5. Ozuku, T.; Ueda, A. *J. Electrochem. Soc*. **1994**, *141*, 2972.
6. Ohzuku, T.; Ueda, A.; Nagayama, M.; Yasunou, Y.; Komori, H. *Electrochim. Acta* **1993**, *38*, 1159.
7. Plichta, E.; Slane, S.; Uchiyama, M.; Solomon, M.; Chua, D.; Ebner, W. B.; Lin, H. W. *J. Electrochem. Soc*. **1989**, *136*, 1865.
8. Antaya, M.; Dahn, J. R.; Preston, J. S.; Rossen, E.; Reimers, J. N. *J. Electrochem. Soc*. **1993**, *140*, 575.
9. Uchida, I.; Sato, H. *J. Electrochem. Soc*. **1995**, *142*, L139.
10. Ogihara, T.; Yanagawa, T.; Ogata, N.; Yoshida, K.; Mizuno, Y.; Yonezawa, S.; Takashima, M.; Nagata, N.; Ogawa, K. *Denki Kagaku* **1993**, *61*, 1339.
11. Yoshio, M.; Tanaka, H.; Tominaga, K.; Naguchi, H. *J. Power Source* **1992**, *40*, 347.
12. Garcia, B.; Farcy, J.; Pereira-Ramos, J. P.; Perichon, J.; Baffier, N. *J. Power Sources* **1995**, *54*, 373.
13. Yazami, R.; Lebrun, N.; Bonneau, M.; Molteni, M. *J. Power Sources* **1995**, *54*, 389.
14. Chang, S. W.; Lee, T. J.; Lin, S. C.; Jeng, J. H. *J. Power Sources* **1995**, *54*, 403.
15. Jeong, E. D.; Won, M. S.; Shim, Y. B. *J. Power Sources* **1998**, *70*, 70.
16. Cho, P. J.; Jeong, E. D.; Shim, Y. B. *Bull Korean Chem. Soc*. **1998**, *19*, 39.
17. Barboux, P.; Tarascon, J. M.; Shokoohi, F. K. *J. Solid State Chem*. **1991**, *94*, 185.
18. Hwang, H.; Bruce, P. G. *J. Elecrochem. Soc*. **1994**, *141*, L106.
19. Bach, S.; Henry, M.; Barrier, N.; Civage, J. *J. Solid State Chem*. **1990**, *88*, 325.
20. Pyun, S. I.; Bae, J. S. *Electrochim. Acta* **1996**, *41*, 919.
21. Choi, Y. M.; Pyun, S. I.; Bae, J. S.; Moon, S. I. *J. Power Sources* **1995**, *56*, 25.
22. Cabanel, R.; Barral, G.; Diard, J. P.; Le Gorrec, B.; Montella, C. *J. Appl. Electrochem*. **1993**, *23*, 93.
23. Thomas, M. G. S. R.; Bruce, P. G.; Goodennough, J. B. *J. Electrochem. Soc*. **1985**, *132*, 1521.
24. Thomas, M. G. S. R.; Bruce, P. G.; Goodennough, J. B. *Solid State Ionics* **1985**, *17*, 13.
25. Pistoia, G.; Zane, D.; Zhang, Y. *J. Electrochem. Soc*. **1995**, *142*, 2551.
26. Nishima, T.; Sato, H.; Uchida, I. *The 36th Battery Symposium in Japan*; 1995; p 7-8.